



# Origin of the RNA world: The fate of nucleobases in warm little ponds

Ben K. D. Pearce<sup>a,b,1</sup>, Ralph E. Pudritz<sup>a,b,c,d</sup>, Dmitry A. Semenov<sup>c</sup>, and Thomas K. Henning<sup>c</sup>

<sup>a</sup>Origins Institute, McMaster University, Hamilton, ON L8S 4M1, Canada; <sup>b</sup>Department of Physics and Astronomy, McMaster University, Hamilton, ON L8S 4M1, Canada; <sup>c</sup>Planet and Star Formation Department, Max Planck Institute for Astronomy, 69117 Heidelberg, Germany; and <sup>d</sup>Institute for Theoretical Astrophysics, Center for Astronomy Heidelberg, 69120 Heidelberg, Germany

Edited by Donald E. Canfield, Institute of Biology and Nordic Center for Earth Evolution, University of Southern Denmark, Odense M., Denmark, and approved August 28, 2017 (received for review June 7, 2017)

Before the origin of simple cellular life, the building blocks of RNA (nucleotides) had to form and polymerize in favorable environments on early Earth. At this time, meteorites and interplanetary dust particles delivered organics such as nucleobases (the characteristic molecules of nucleotides) to warm little ponds whose wet-dry cycles promoted rapid polymerization. We build a comprehensive numerical model for the evolution of nucleobases in warm little ponds leading to the emergence of the first nucleotides and RNA. We couple Earth's early evolution with complex prebiotic chemistry in these environments. We find that RNA polymers must have emerged very quickly after the deposition of meteorites (less than a few years). Their constituent nucleobases were primarily meteoritic in origin and not from interplanetary dust particles. Ponds appeared as continents rose out of the early global ocean, but this increasing availability of "targets" for meteorites was offset by declining meteorite bombardment rates. Moreover, the rapid losses of nucleobases to pond seepage during wet periods, and to UV photodissociation during dry periods, mean that the synthesis of nucleotides and their polymerization into RNA occurred in just one to a few wet-dry cycles. Under these conditions, RNA polymers likely appeared before 4.17 billion years ago.

life origins | astrobiology | planetary science | meteoritics | RNA world

One of the most fundamental questions in science is how life first emerged on Earth. Given its ubiquity in living cells and its ability to both store genetic information and catalyze its own replication, RNA probably formed the basis of first life (1). RNA molecules are made up of sequences of four different nucleotides, the latter of which can be formed through reaction of a nucleobase with a ribose and a reduced phosphorous (P) source (2, 3). The evidence suggests that first life appeared earlier than 3.7 Gy ago (Ga) (4, 5), and thus the RNA world would have developed on a violent early Earth undergoing meteoritic bombardment at a rate of  $\sim 1$  to  $1,000 \times 10^{12}$  kg/y (6), which is  $\sim 8$  to 11 orders of magnitude greater than today (7). At that time, the atmosphere was dominated by volcanic gases, and dry land was scarce as continents were rising out of the global ocean. What was the source of the building blocks of RNA? What environments enabled nucleotides to polymerize and form the first functioning RNA molecules under such conditions? Although experiments have produced simple RNA strands in highly idealized laboratory conditions (8, 9), the answers to these questions are largely unknown.

As to the sources of nucleobases, early Earth's atmosphere was likely dominated by CO<sub>2</sub>, N<sub>2</sub>, SO<sub>2</sub>, and H<sub>2</sub>O (10). In such a weakly reducing atmosphere, Miller-Urey-type reactions are not very efficient at producing organics (11). One solution is that the nucleobases were delivered by interplanetary dust particles (IDPs) and meteorites. During these early times, these bodies delivered  $\sim 6 \times 10^7$  and  $\sim 2 \times 10^3$  kg·y<sup>-1</sup> of intact carbon, respectively (11). Although nucleobases have not been identified in IDPs, three of the five nucleobases (uracil, cytosine, and thymine) have been formed on the surfaces of icy IDP ana-

logues in the laboratory through exposure to UV radiation (12). Nucleobases are found in meteorites (guanine, adenine, and uracil) with concentrations of 0.25 to 515 parts per billion (ppb) (13, 14). The ultimate source of nitrogen within them could be molecules such as ammonia and HCN that are observed in the disks of gas and dust around all young stars (15–17). A second possible source of nucleobases is synthesis in hydrothermal vents that well up from spreading cracks on young Earth's ocean floors (18). A potential problem here is the lack of concentrated and reactive nitrogen sources in these environments (18).

A central question concerning the emergence of the RNA world is how the polymerization of nucleotides occurred. Warm little ponds (WLPs) are excellent candidate environments for this process because their wet and dry cycles have been shown to promote the polymerization of nucleotides into chains possibly greater than 300 links (8). Furthermore, clay minerals in the walls and bases of WLPs promote the linking of chains up to 55 nucleotides long (19). Conversely, experiments simulating the conditions of hydrothermal vents have only succeeded in producing RNA chains a few monomers long (20). A critical problem for polymerizing long RNA chains near hydrothermal vents is the absence of wet-dry cycles.

## Model: Fates of Nucleobases in Evolving WLPs

We compute a well-posed model for the evolution of WLPs, the fates of nucleobases delivered to them, and the emergence of RNA polymers under early Earth conditions. The sources of nucleobases in our model are carbonaceous meteorites and IDPs whose delivery rates are estimated using the lunar cratering record (6, 11, 21), the distribution of asteroid masses (21), and the fraction of meteorites reaching terminal velocity that are known to be nucleobase carriers (13,

## Significance

There are currently two competing hypotheses for the site at which an RNA world emerged: hydrothermal vents in the deep ocean and warm little ponds. Because the former lacks wet and dry cycles, which are well known to promote polymerization (in this case, of nucleotides into RNA), we construct a comprehensive model for the origin of RNA in the latter sites. Our model advances the story and timeline of the RNA world by constraining the source of biomolecules, the environmental conditions, the timescales of reaction, and the emergence of first RNA polymers.

Author contributions: B.K.D.P., R.E.P., D.A.S., and T.K.H. designed research; B.K.D.P. performed research; B.K.D.P. and R.E.P. analyzed data; and B.K.D.P., R.E.P., D.A.S., and T.K.H. wrote the paper.

The authors declare no conflict of interest.

This article is a PNAS Direct Submission.

See Commentary on page 11264.

<sup>1</sup>To whom correspondence should be addressed. Email: pearcbe@mcmaster.ca.

This article contains supporting information online at [www.pnas.org/lookup/suppl/doi:10.1073/pnas.1710339114/-DCSupplemental](http://www.pnas.org/lookup/suppl/doi:10.1073/pnas.1710339114/-DCSupplemental).

22). The WLPs are “targets” in which molecular evolution of nucleobases into nucleotides and subsequent polymerization into RNA occur. The evolution of ponds due to precipitation, evaporation, and seepage constitutes the immediate environments in which the delivered nucleobases must survive and polymerize. [We don’t emphasize groundwater-fed ponds (hot springs) because their small number on Earth today—approximately thousands—compared with regular lakes/ponds— $\sim$ 304 million (23)—suggests they didn’t contribute greatly to the combined WLP target area for meteorite deposition.] The data for these sources and sinks are gathered from historical precipitation records (24), or are measured experimentally (25, 26). Sinks for these molecules include destruction by unattenuated UV rays (as early Earth had no ozone), hydrolysis in the pond water, as well as seepage from the bases of ponds. The data for these sinks are measured experimentally (26–28). The nucleobases that survive go on to form nucleotides that ultimately polymerize.

To calculate the number of carbonaceous meteorite source depositions in target WLPs on early Earth, we combine a continental crustal growth model (29), the lake and pond size distribution and ponds per unit crustal area estimated for ponds on Earth today (23), the asteroid belt mass distribution (21), and three possible mass delivery models based on the lunar cratering record (6, 21). This results in a first-order linear differential equation (Eq. S18), which we solve analytically. The details are in *SI Text*, and the main results are discussed in *Meteorite Sources and Targets*.

Nucleobase abundances in WLPs from IDPs and meteorites are described in our model by first-order linear differential equations (Eqs. S34 and S38, respectively). The equations are solved numerically (see *SI Text* for details).

Our fiducial model WLPs are cylindrical (because sedimentation flattens their initial bases) and have a 1-m radius and depth. We find these ponds to be optimal because they are large enough

to not dry up too quickly but small enough that high nucleobase concentrations can be achieved (see *SI Text*).

## Meteorite Sources and Targets

In Fig. 1A, we show the history of meteoritic mass delivery rates on early Earth, and of WLP targets. From total meteoritic mass, we extract just the nucleobase sources, i.e., only carbonaceous meteoroids whose fragments slow to terminal velocity in the early atmosphere. In Fig. 1B, we show the history of depositions of such nucleobase sources into 1- to 10-m-radius WLP targets from 4.5 Ga to 3.7 Ga.

The lunar cratering record either shows a continuously decreasing rate of impacts from 4.5 Ga forward or shows a brief outburst beginning at  $\sim$ 3.9 Ga known as the Late Heavy Bombardment (LHB). Due to the lack of lunar impact melts with ages before  $\sim$ 3.92 Ga, the rate of mass delivered to early Earth preceding this date is uncertain (30). Therefore, we compare three models for mass delivery to early Earth based on analytical fits to the lunar cratering record (6, 21): an LHB and a minimum and a maximum bombardment model. The latter two models represent lower and upper limit fits for a sustained declining bombardment, and are subject to considerable uncertainty (31). The total target area of WLPs increases as the rising continents provide greater surface area for pond sites. An ocean world, in this view, is an implausible environment for the emergence of an RNA world. Iron and rocky bodies impact the solid surface at speeds high enough to form small craters (32), contributing to the WLP population.

Our calculations show that 10 to 3,840 terminal velocity carbon-rich meteoroids would have deposited their fragments into WLPs on Earth during the Hadean Eon. Given the large uncertainty of the ponds per unit area and the growth rate of continental crust, we vary the WLP growth function by  $\pm 1$  order of magnitude. From this, we get a minimum of 1 to 384 depositions and a maximum of 100 to 38,400 WLP depositions from 4.5 Ga to 3.7 Ga. The optimal model for WLP depositions—the

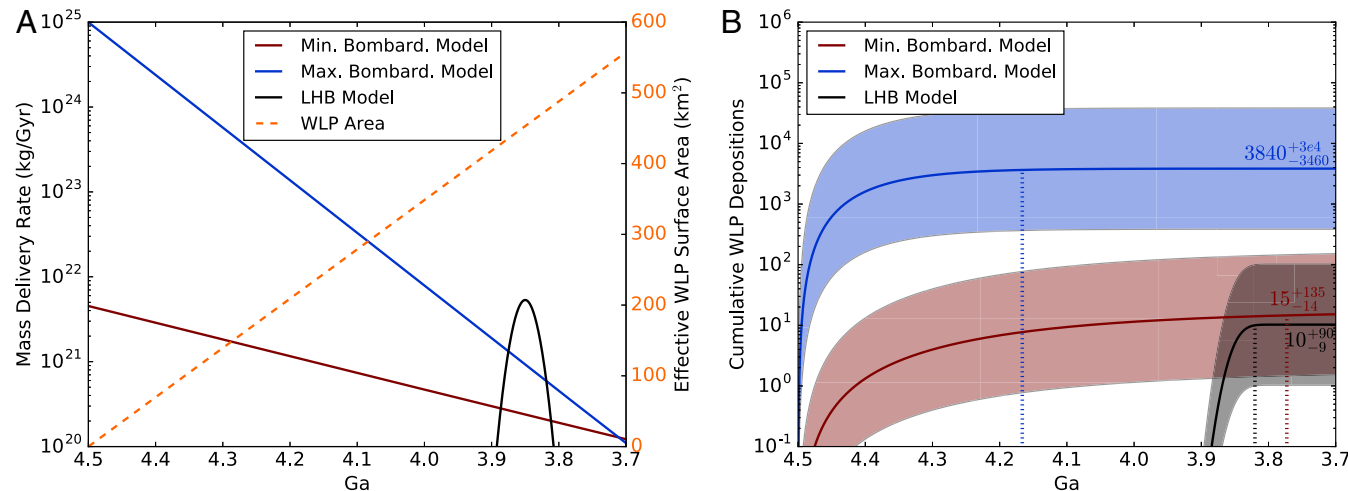


**Fig. 1.** History of carbonaceous meteorite deposition in WLPs. (A) History of mass delivery rate to early Earth and of effective WLP surface area. Three models for mass delivered to early Earth are compared: an LHB model and a minimum and a maximum bombardment model. All mass delivery models are based on analyses of the lunar cratering record (6, 21). The effective WLP surface area during the Hadean Eon is based on a continental crust growth model (29), the number of lakes and ponds per unit crustal area (23), and the lake and pond size distribution (23). (B) Cumulative WLP depositions for the small fragments of carbonaceous meteoroids of diameter 40 m to 80 m landing in any 1- to 10-m-radius WLP on early Earth. A deposition is characterized as a meteoroid debris field that overlaps with a WLP. We assume the ponds per area during the Hadean Eon is the same as today, and that all continental crust remains above sea level; however, we vary the ponds per area by plus or minus one order of magnitude to obtain error bars. Ninety-five percent of WLP depositions in each model occur before the corresponding dotted vertical line; 40 m to 80 m is the optimal range of carbonaceous meteoroid diameters to reach terminal velocity, while still landing a substantial fraction of mass within a WLP area; and 1 m to 10 m is the optimal range of WLP radii to avoid complete evaporation within a few months, while also allowing nonnegligible nucleobase concentrations to be reached upon meteorite deposition. The numbers of carbonaceous meteoroid impactors in the 20- to 40-m-radius range are based on the mass delivery rate, the main-belt size-frequency distribution, and the fraction of impactors that are Mighei type, Renazzo type, or Ivuna type (6, 21, 22) (see *SI Text*).

maximum bombardment model—suggests the majority of depositions occurred before 4.17 Ga. The less optimal models for WLP depositions, the LHB and minimum bombardment models, suggest the majority of depositions occurred before 3.82 Ga and 3.77 Ga, respectively.

### Life Cycles of WLPs

Fig. 2 illustrates the variation of physical conditions for WLPs during the Hadean Eon, ~4.5 Ga to 3.7 Ga. Annual rainfall varies sinusoidally (24), creating seasonal wet and dry environments. The increased heat flow from greater abundances of radiogenic sources at this time (33) causes temperatures of around 50 °C to 80 °C (34). The various factors that control the water level and thus the wet–dry cycles of WLPs are precipitation, evaporation, and seepage (through pores in the ground).

In Fig. 3A, we present the results of these calculations. We select two different temperatures (65 °C and 20 °C) as analogues for hot and warm early Earths. For each of these, we examine three different environments: dry, intermediate, and wet (see Table 1 for details). The water levels in the wet environment WLPs range from ~60 to 100% full. WLPs experiencing dry states of approximately half (intermediate environment) and three quarters of a year (dry environment) only fill up to 20% and 10%, respectively. These results clearly establish the existence of seasonal wet–dry cycles.

### Nucleobase Evolution in WLPs

As shown in Fig. 2, the buildup of nucleobases in WLPs is offset by losses due to hydrolysis (28), seepage (26), and dissociation by

UV radiation that was incident on early Earth in the absence of ozone (27, 36). Some protection would be afforded during WLP wet phases, as a 1-m column of pond water can absorb UV radiation up to ~95% (37). It is of particular interest that sediment, which collects at the base of WLPs, also attenuates UV radiation. Studies show it only takes a ~0.6-mm layer of basaltic sediment to attenuate UV radiation by >99.99% (38).

Nucleotide formation and stability are sensitive to temperature. Phosphorylation of nucleosides in the laboratory is slower at low temperatures, taking a few weeks at 65 °C compared with a couple of hours at 100 °C (39). The stability of nucleotides on the other hand, is favored in warm conditions over high temperatures (40). If a WLP is too hot (>80 °C), any newly formed nucleotides within it will hydrolyze in several days to a few years (40). At temperatures of 5 °C to 35 °C that either characterize more-temperate latitudes or a postsnowball Earth, nucleotides can survive for thousand-to-million-year timescales. However, at such temperatures, nucleotide formation would be very slow. Considering this temperature sensitivity, we model the evolution of nucleobases in WLPs in matching warm (5 °C to 35 °C) and hot (50 °C to 80 °C) early Earth environments. Hotter ponds evaporate more quickly; therefore, we choose rainier analogue sites on a hot early Earth to maintain identical pond environments to our warm early Earth sites.

In Fig. 3B, we focus on the adenine concentrations in WLPs from only IDP sources. The combination of spikes, flat tops, and troughs in Fig. 3B reflects the variations of adenine concentration in response to drying, balance of input and destruction rates, and precipitation during wet periods. In any environment

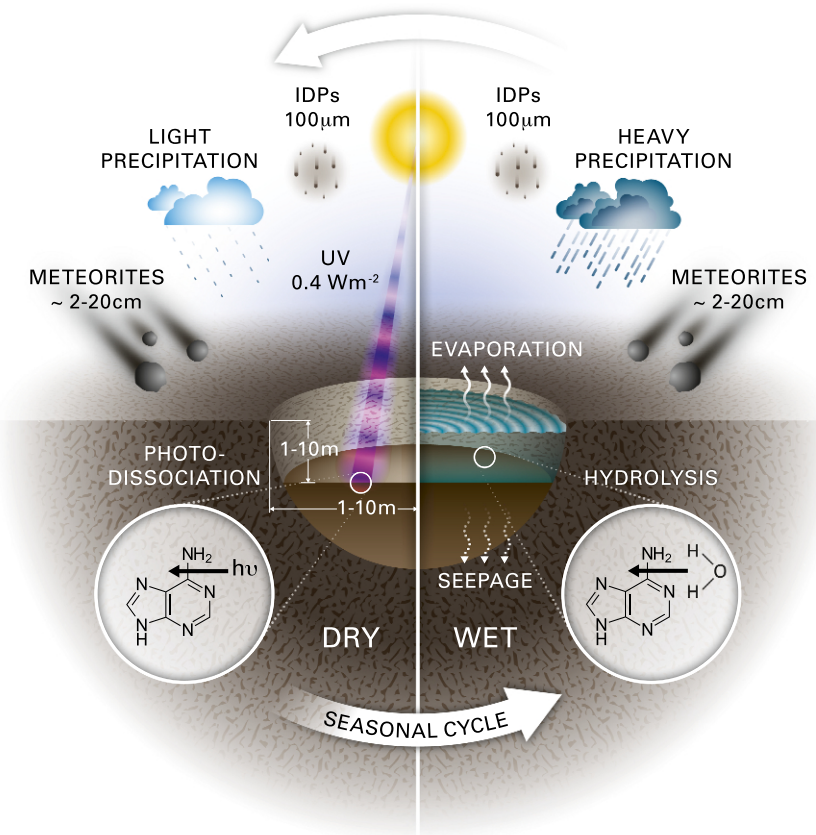


**Fig. 2.** An illustration of the sources and sinks of pond water and nucleobases in our model of isolated WLPs on early Earth. The only water source is precipitation. Water sinks include evaporation and seepage. Nucleobase sources include carbonaceous IDPs and meteorites, which carry up to ~1 pg and ~3 mg, respectively, of each nucleobase. Nucleobase sinks include hydrolysis, UV photodissociation, and seepage. Nucleobase hydrolysis and seepage are only activated when the pond is wet, and UV photodissociation is only activated when the pond is dry.

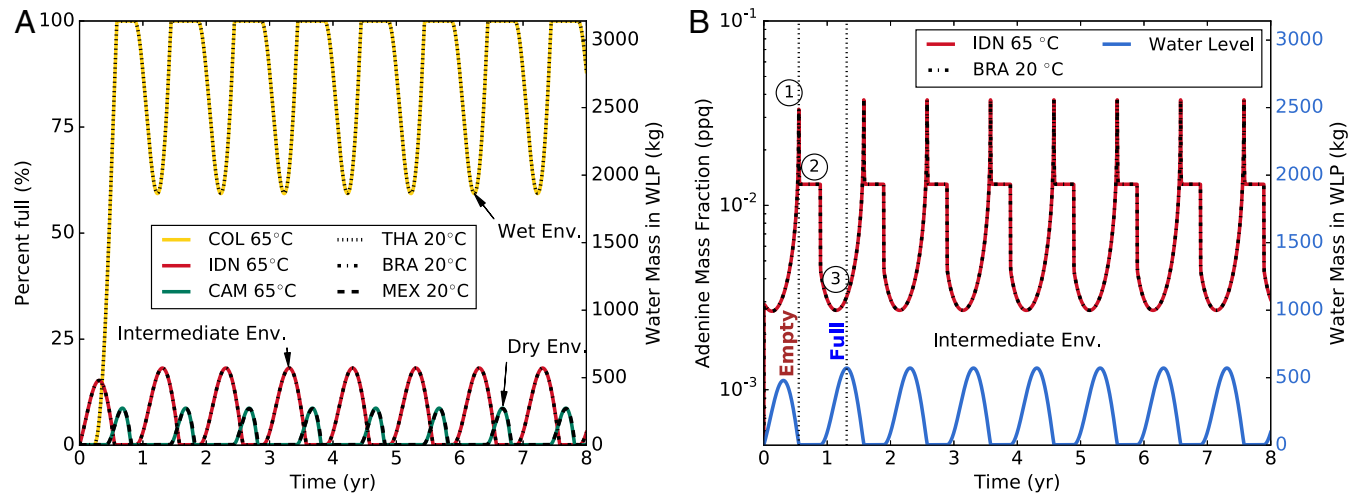


**Fig. 3.** Histories of pond water and adenine concentration from IDPs. (A) The change in water level over time in our fiducial dry, intermediate, and wet environment WLPs due to evaporation, seepage, and precipitation. Precipitation rates from a variety of locations on Earth today are used in the models, and represent two classes of matching early Earth analogues: hot (Columbia, Indonesia, Cameroon) and warm (Thailand, Brazil, and Mexico) (for details, see Table 1). All models begin with an empty pond, and stabilize within 2 y. (B) The red and black-dotted curves represent the adenine concentrations over time from carbonaceous IDPs in our fiducial WLPs. The degenerate intermediate WLP environment used in this calculation is for a hot early Earth at 65 °C and a warm early Earth at 20 °C. The blue curve represents the corresponding water level in the WLP, with initial empty and full states labeled vertically. Three features are present: (1) the maximum adenine concentration at the onset of the dry phase, (2) a flat-top equilibrium between incoming adenine from IDPs and adenine destruction by UV irradiation, and (3) the minimum adenine concentration just before the pond water reaches its highest level. BRA, Brazil; CAM, Cameroon; COL, Columbia; Env, environment; IDN, Indonesia; MEX, Mexico; THA, Thailand.

and at any modeled temperature, the maximum adenine concentration from only IDP sources remains below  $2 \times 10^{-7}$  ppb (Fig. S1). This is two orders of magnitude below current detection limits (14), making subsequent reactions negligible. The nucleobase mass fraction curves are practically independent of pond size ( $1 \text{ m} < r_p \leq 10 \text{ m}$ ) once a stable, seasonal pattern is reached (<35 y). This is because, although larger ponds have a larger collecting area for IDPs, they have an equivalent larger area for collecting precipitation and seeping nucleobases.

### Dominant Source of Surviving Nucleobases

In Fig. 4, we assemble all of these results and compare carbonaceous IDPs to meteorites as sources of adenine to our fiducial WLPs. Small meteorite fragments (1 cm in radius) are compared with IDPs in Fig. 4A. The effects of larger meteorite fragments (5 cm and 10 cm) on adenine concentration are displayed in Fig. 4B.

The maximum adenine concentration in our model WLPs from carbonaceous meteorites is 10 orders of magnitude higher than the maximum adenine concentration from carbonaceous IDPs. The reason for this huge disparity is simply that carbonaceous meteoroid fragments—each carrying up to a few milligrams of adenine—are deposited into a WLP in a single event. This allows adenine to reach parts per billion–parts per million-level concentrations before seepage and UV photodissociation efficiently remove it from the WLP in one to a few wet–dry cycles. The maximum guanine and uracil accumulated in our model WLPs from meteorites are also more than 10 orders of magnitude higher than those accumulated from IDPs (Figs. S2 and S3). A maximum adenine concentration of 2 ppm is still approximately one to two orders of magnitude lower than the initial adenine concentrations in aqueous experiments forming adenosine and AMP (2); however, these experiments only ran for an hour.

Adenine within larger fragments diffuses over several wet–dry cycles, and, during the dry phase, no outflow occurs. For fragments 1, 5, and 10 cm in radius, 99% of the adenine is released into the pond water within ~10 d, 8 mo, and 32 mo, respectively

(Fig. S4). Only the adenine that has already flowed out of the fragments gets rapidly photodestroyed; therefore, adenine within larger fragments can survive up to ~7 y.

Thus, even though the carbon delivery rates from IDPs to early Earth vastly exceed those from meteorites, it is the meteoritic material that is the dominant source of nucleobases for RNA synthesis.

### Nucleotide and RNA Synthesis

To form nucleotides in WLPs, ribose and a reduced P source must be available. Ribose may have formed and stabilized in borate-rich WLPs via the formose reaction (polymerization of H<sub>2</sub>CO) (41). Additionally, phosphite has been detected in a pristine geothermal pool representative of early Earth, suggesting the potential availability of reduced P to WLP environments

**Table 1.** Precipitation models matching dry, intermediate, and wet environments on a warm (5 °C to 35 °C) and hot (50 °C to 80 °C) early Earth

Model	Environment	Analogue site	$\bar{P}, \text{m}\cdot\text{y}^{-1}$	$\delta_p$	$s_p$
Warm early Earth (5 °C to 35 °C)	Dry	Mexico (MEX)	0.94	1.69	0.3
	Intermediate	Brazil (BRA)	1.8	0.50	0.85
	Wet	Thailand (THA)	3.32	0.91	0.3
Hot early Earth (50 to 80 °C)	Dry	Cameroon (CAM)	3.5	0.5	0.3
	Intermediate	Indonesia (IDN)	4.5	0.2	0.85
	Wet	Columbia (COL)	6.0	0.5	0.3

Precipitation data from a variety of locations on Earth today (24, 35) represent two classes of matching early Earth analogues: warm (Thailand, Brazil, and Mexico) and hot (Columbia, Indonesia, Cameroon). For example, the conditions in Mexico on a warm early Earth match the conditions in Cameroon on a hot early Earth.  $\bar{P}$  is the mean precipitation rate,  $\delta_p$  is the seasonal precipitation amplitude, and  $s_p$  is the phase shift. To obtain the rate of the decrease in pond water for a given analogue site, table values are input into this equation:  $dL/dt = 0.83 + 0.06T - \bar{P}[1 + \delta_p \sin(2\pi(t - s_p)/\tau_s)]$  (see SI Text).

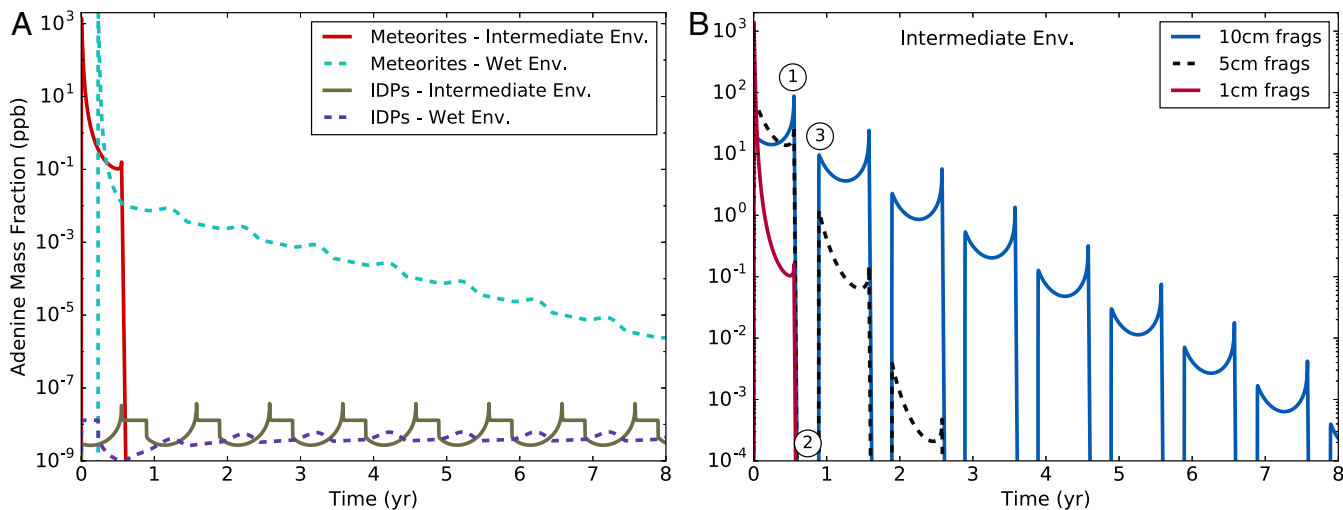


**Fig. 4.** Comparative histories of adenine concentrations from IDPs and meteorites. (A) A comparison of the accumulation of adenine from carbonaceous IDPs and meteorites in our fiducial WLPs. The meteorite fragments are small (1 cm), and originate from a 40-m-radius carbonaceous meteoroid. Adenine concentrations for intermediate (wet-dry cycle) and wet environments (never dry) are compared and correspond to both a hot early Earth at 65 °C and a warm early Earth at 20 °C (for details, see Table 1). (B) The effect of meteorite fragment sizes on adenine concentration. The degenerate intermediate WLP environment used in these calculations is for a hot early Earth at 65 °C and a warm early Earth at 20 °C. The fragments are either only small in size (1 cm in radius), only medium in size (5 cm in radius), or only large in size (10 cm in radius). Three features are present: (1) Adenine is at its highest concentration at the onset of the pond's dry phase. (2) Upon drying, adenine ceases to outflow from large fragments, and UV radiation rapidly destroys all previously released adenine. (3) Rewetting allows the remaining adenine within large fragment pores to continue to outflow. The U shape is due to the increase and decrease in water level. Env., environment.

(42). Only the AMP nucleotide has been experimentally synthesized in a single step involving ribose, reduced P, and UV radiation (2).

Because of the rapid rate of seepage [ $\sim 1.0 \text{ mm} \cdot \text{d}^{-1}$  to  $5.1 \text{ mm} \cdot \text{d}^{-1}$  (26)], nucleotide synthesis would need to be fast, occurring within a half-year to a few years after nucleobase deposition, depending on meteoroid fragment sizes. This is ample time given that laboratory experiments show that hour-to-week-long timescales are sufficient to form adenosine and AMP (2, 3).

Nucleotides, once synthesized using meteorite-delivered nucleobases, are still subject to seepage, regardless of the temperature. Therefore, nucleotide polymerization into RNA would also need to be fast, occurring within one to a few wet-dry cycles, to reduce their likelihood of seeping through the estimated 0.001- to 400-μm-sized pores at the WLP base (43). Experiments show that nucleotides can polymerize into RNA chains possibly greater than 300 monomers by subjecting them to just 1 to 16 wet-dry cycles (8).

## Discussion and Conclusions

Seepage is one of the dominant nucleobase sinks in WLPs. It will be drastically reduced if nucleobases are encapsulated by vesicles (spheres of size 0.5 μm to 5 μm that form spontaneously upon hydration, whose walls consist of lipid bilayers derived from fatty acids within meteorites) (44). However, even if seepage is turned off, maximum adenine concentrations from IDPs are still negligible [ $\lesssim 150 \text{ ppq}$  (parts per quadrillion)] (Fig. S5).

Also, we note that a cold early Earth [if it occurred (30)] with seasonal or impact-induced freeze-thaw cycles could also be suitable for RNA polymerization and evolution for reasons similar to

those we have analyzed for WLPs. The cyclic thawing and freezing resembles wet-dry cycles (8).

We conclude that the physical and chemical conditions of WLPs place strong constraints on the emergence of an RNA world. A hot early Earth (50 °C to 80 °C) favors rapid nucleotide synthesis in WLPs (39). Meteorite-delivered nucleobases could react with ribose and a reduced P source to quickly (less than a few years) create nucleotides for polymerization. Polymerization then occurs in one to a few wet-dry cycles to reduce the likelihood that these molecules are lost to seepage. This rapid process also reduces the likelihood of setbacks for the emergence of the RNA world due to frequent large impacts, also known as impact frustration (45). Sedimentation would be of critical importance as UV protection for nucleobases, nucleotides, and RNA (27, 46, 47).

The mass delivery model providing the most WLP depositions indicates that the majority of meteorite depositions occurred before 4.17 Ga. The first RNA polymers would have formed in WLPs around that time, prefiguring the emergence of the RNA world. This implies that the RNA world could have appeared within ~200 to 300 million years after Earth became habitable.

**ACKNOWLEDGMENTS.** We thank the referees for their thoughtful insights. We thank M. Rheinstädter for providing valuable comments on the manuscript. B.K.D.P. thanks the Max Planck Institute for Astronomy for their hospitality during his summer abroad, supported by a Natural Sciences and Engineering Research Council of Canada (NSERC) Michael Smith Foreign Study Supplement. R.E.P. thanks the Max Planck Institute for Astronomy and the Institute of Theoretical Astrophysics for their support during his sabbatical leave. The research of B.K.D.P. was supported by an NSERC Canada Graduate Scholarship and Ontario Graduate Scholarship. R.E.P. is supported by an NSERC Discovery Grant. This research is part of a collaboration between the Origins Institute and the Heidelberg Initiative for the Origins of Life.

1. Gilbert W (1986) Origin of life: The RNA world. *Nature* 319:618.
2. Ponnamperuma C, Sagan C, Mariner R (1963) Synthesis of adenosine triphosphate under possible primitive Earth conditions. *Nature* 199:222–226.
3. Gull M, et al. (2015) Nucleoside phosphorylation by the mineral schreibersite. *Sci Rep* 5:17198.
4. Nutman AP, Bennett VC, Friend CRL, Van Kranendonk MJ, Chivas AR (2016) Rapid emergence of life shown by discovery of 3,700-million-year-old microbial structures. *Nature* 537:535–538.
5. Ohtomo Y, Kakegawa T, Ishida A, Nagase T, Rosing MT (2014) Evidence for biogenic graphite in early Archaean Isua metasedimentary rocks. *Nat Geosci* 7:25–28.

6. Chyba CF (1990) Impact delivery and erosion of planetary oceans in the early inner solar system. *Nature* 343:129–133.
7. Bland PA, et al. (1996) The flux of meteorites to the Earth over the last 50,000 years. *Mon Not R Astron Soc* 283:551–565.
8. Da Silva L, Maurel MC, Deamer D (2015) Salt-promoted synthesis of RNA-like molecules in simulated hydrothermal conditions. *J Mol Evol* 80:86–97.
9. Orgel LE (2004) Prebiotic chemistry and the origin of the RNA world. *Crit Rev Biochem Mol Biol* 39:99–123.
10. Trail D, Watson EB, Tailby ND (2011) The oxidation state of Hadean magmas and implications for early Earth's atmosphere. *Nature* 480:79–82.
11. Chyba C, Sagan C (1992) Endogenous production, exogenous delivery and impact-shock synthesis of organic molecules: An inventory for the origins of life. *Nature* 355:125–132.
12. Nuevo M, Materese CK, Sandford SA (2014) The photochemistry of pyrimidine in realistic astrophysical ices and the production of nucleobases. *Astrophys J* 793:125.
13. Pearce BKD, Pudritz RE (2015) Seeding the pregenetic Earth: Meteoritic abundances of nucleobases and potential reaction pathways. *Astrophys J* 807:85.
14. Callahan MP, et al. (2011) Carbonaceous meteorites contain a wide range of extraterrestrial nucleobases. *Proc Natl Acad Sci USA* 108:13995–13998.
15. Pearce BKD, Pudritz RE (2016) Meteorites and the RNA world: A thermodynamic model of nucleobase synthesis within planetesimals. *Astrobiology* 16:853–872.
16. Salinas VN, et al. (2016) First detection of gas-phase ammonia in a planet-forming disk.  $\text{NH}_3$ ,  $\text{N}_2\text{H}^+$ , and  $\text{H}_2\text{O}$  in the disk around TW Hydrae. *Astron Astrophys* 591:A122.
17. Pasucci I, et al. (2009) The different evolution of gas and dust in disks around Sun-like and cool stars. *Astrophys J* 696:143–159.
18. Schoonen MAA, Xu Y (2001) Nitrogen reduction under hydrothermal vent conditions: Implications for the prebiotic synthesis of C-H-O-N compounds. *Astrobiology* 1:133–142.
19. Ferris JP, Hill AR, Liu R, Orgel LE (1996) Synthesis of long prebiotic oligomers on mineral surfaces. *Nature* 381:59–61.
20. Burcar BT, et al. (2015) RNA oligomerization in laboratory analogues of alkaline hydrothermal vent systems. *Astrobiology* 15:509–522.
21. Abramov O, Mojzsis SJ (2009) Microbial habitability of the Hadean Earth during the late heavy bombardment. *Nature* 459:419–422.
22. Burbine TH, McCoy TJ, Meibom A, Gladman B, Keil K (2002) *Meteoritic Parent Bodies: Their Number and Identification*, eds Bottke WF, Jr, Cellino A, Paolicchi P, Binzel RP (Univ Ariz Press, Tucson, AZ), pp 653–667.
23. Downing JA, et al. (2006) The global abundance and size distribution of lakes, ponds, and impoundments. *Limnol Oceanogr* 51:2388–2397.
24. Berghuijs WR, Woods RA (2016) A simple framework to quantitatively describe monthly precipitation and temperature climatology. *Int J Climatol* 36:3161–3174.
25. Boyd CE (1985) Pond evaporation. *Trans Am Fish Soc* 114:299–303.
26. Boyd CE (1982) Hydrology of small experimental fish ponds at Auburn, Alabama. *Trans Am Fish Soc* 111:638–644.
27. Poch O, et al. (2015) Effect of nontronite smectite clay on the chemical evolution of several organic molecules under simulated martian surface ultraviolet radiation conditions. *Astrobiology* 15:221–237.
28. Levy M, Miller SL (1998) The stability of the RNA bases: Implications for the origin of life. *Proc Natl Acad Sci USA* 93:7933–7938.
29. McCulloch MT, Bennett VC (1993) Evolution of the early Earth: Constraints from  $^{143}\text{Nd}$ - $^{142}\text{Nd}$  isotopic systematics. *Lithos* 30:237–255.
30. Zahnle K, et al. (2007) Emergence of a habitable planet. *Space Sci Rev* 129:35–78.
31. Chyba CF (1991) Terrestrial mantle siderophiles and the lunar impact record. *Icarus* 92:217–233.
32. Hills JG, Goda MP (1993) The fragmentation of small asteroids in the atmosphere. *Astron J* 105:1114–1144.
33. Sleep NH (2010) The Hadean-Archaean environment. *Cold Spring Harbor Perspect Biol* 2:a002527.
34. Cockell CS (2015) *Astrobiology: Understanding Life in the Universe* (Wiley, Chichester, UK).
35. Reichle RH, et al. (2011) Assessment and enhancement of MERRA land surface hydrology estimates. *J Clim* 24:6322–6338.
36. Rugheimer S, Segura A, Kaltenegger L, Sasselov D (2015) UV surface environment of Earth-like planets orbiting FGKM stars through geological evolution. *Astrophys J* 806:137.
37. Wozniak B, Dera J (2007) Light absorption by water molecules and inorganic substances dissolved in sea water. *Light Absorption in Sea Water*, Atmospheric and Oceanographic Sciences Library (Springer, New York), Vol 33, pp 11–81.
38. Carrier BL, Beegle LW, Bhartia R, Abbey WJ (2017) Attenuation of UV radiation in rocks and minerals: Implications for biosignature preservation and detection on Mars. *Lunar Planet Sci Conf* 48:2678.
39. Handschuh GJ, Lohrmann R, Orgel LE (1973) The effect of  $\text{Mg}^{2+}$  and  $\text{Ca}^{2+}$  on urea-catalyzed phosphorylation reactions. *J Mol Evol* 2:251–262.
40. Hulett HR (1970) Non-enzymatic hydrolysis of adenosine phosphates. *Nature* 225:1248–1249.
41. Furukawa Y, Horiuchi M, Kakegawa T (2013) Selective stabilization of ribose by borate. *Orig Life Evol Biosph* 43:353–361.
42. Pech H, et al. (2009) Detection of geothermal phosphite using high-performance liquid chromatography. *Environ Sci Technol* 43:7671–7675.
43. Tugrul A (1997) Change in pore size distribution due to weathering of basalts and its engineering significance. *Proceedings: International Symposium on Engineering Geology and the Environment*, eds Marinos PG, Koukis GC, Tsiambaos GC, Stouras GC (Balkema, Rotterdam), Vol 1, pp 71–90.
44. Damer B, Deamer DW (2015) Coupled phases and combinatorial selection in fluctuating hydrothermal pools: A scenario to guide experimental approaches to the origin of cellular life. *Life* 5:872–887.
45. Zahnle K, Sleep NH (2006) Impacts and the early evolution of life. *Comets and the Origin and Evolution of Life*, eds Thomas PJ, Hicks RD, Chyba CF, McKay CP (Springer, Berlin), pp 207–251.
46. Dodonova NY, Kiseleva MN, Remisova LA, Tsyganenko NM (1982) The vacuum ultraviolet photochemistry of nucleotides. *Photochem Photobiol* 35:129–132.
47. Kladwang W, Hum J, Das R (2012) Ultraviolet shadowing of RNA can cause significant chemical damage in seconds. *Sci Rep* 2:517.
48. Van Kranendonk MJ (2010) Two types of Archean continental crust: Plume and plate tectonics on early Earth. *Am J Sci* 310:1187–1209.
49. Kenkmann T, et al. (2009) The Carancas meteorite impact crater, Peru: Geologic surveying and modeling of crater formation and atmospheric passage. *Meteoritics* 44:985–1000.
50. Clarke RS, Jr, et al. (1971) The Allende, Mexico, meteorite shower. *Smithson Contrib Earth Sci* 5:1–53.
51. Strom RG, Malhotra R, Ito T, Yoshida F, Kring DA (2005) The origin of planetary impactors in the inner solar system. *Science* 309:1847–1850.
52. Bottke WF, et al. (2005) The fossilized size distribution of the main asteroid belt. *Icarus* 175:111–140.
53. Ehrenfreund P, Glavin DP, Botta O, Cooper G, Bada JL (2001) Special feature: Extraterrestrial amino acids in Orgueil and Ivuna: Tracing the parent body of CI type carbonaceous chondrites. *Proc Natl Acad Sci USA* 98:2138–2141.
54. Weisstein EW (2002) *CRC Concise Encyclopedia of Mathematics* (CRC, Boca Raton, FL), 2nd Ed.
55. Lang B, Kowalski M (1971) On the possible number of mass fragments from Pultusk meteorite shower, 1868. *Meteoritics* 6:149–158.
56. Consolmagno GJ, Macke RJ, Rochette P, Britt DT, Gattaccea J (2006) Density, magnetic susceptibility, and the characterization of ordinary chondrite falls and showers. *Meteoritics* 41:331–342.
57. Bouanna C, Franck S, von Bloh W (2001) The fate of Earth's ocean. *Hydrocl Earth Syst Sci* 5:569–575.
58. Evans NL, Bennett CJ, Ullrich S, Kaiser RI (2011) On the interaction of adenine with ionizing radiation: Mechanistic studies and astrobiological implications. *Astrophys J* 730:69.
59. Kua J, Bada JL (2011) Primordial ocean chemistry and its compatibility with the RNA world. *Orig Life Evol Biosph* 41:553–558.
60. Cockell CS (2002) *The Ultraviolet Radiation Environment of Earth and Mars: Past and Present*, eds Horneck G, Baumstark-Khan C (Springer, Berlin), pp 219–232.
61. Corrigan CM, et al. (1997) The porosity and permeability of chondritic meteorites and interplanetary dust particles. *Meteoritics* 32:509–515.
62. Matrajt G, Brownlee D, Sadilek M, Kruse L (2006) Survival of organic phases in porous IDPs during atmospheric entry: A pulse-heating study. *Meteoritics* 41:903–911.
63. Bland PA, et al. (2009) Why aqueous alteration in asteroids was isochemical: High porosity  $\neq$  high permeability. *Earth Planet Sci Lett* 287:559–568.
64. Palguta J, Schubert G, Travis BJ (2010) Fluid flow and chemical alteration in carbonaceous chondrite parent bodies. *Earth Planet Sci Lett* 296:235–243.
65. Saripalli KP, Serne RJ, Meyer PD, McGrail BP (2002) Prediction of diffusion coefficients in porous media using tortuosity factors based on interfacial areas. *Ground Water* 40:346–352.
66. van Brakel J, Heertjes PM (1974) Analysis of diffusion in macroporous media in terms of a porosity, a tortuosity and a constrictivity factor. *Int J Heat Mass Transfer* 17:1093–1103.
67. Caré S (2003) Influence of aggregates on chloride diffusion coefficient into mortar. *Cem Conc Res* 33:1021–1028.
68. Boving TB, Grathwohl P (2001) Tracer diffusion coefficients in sedimentary rocks: Correlation to porosity and hydraulic conductivity. *J Contam Hydrol* 53:85–100.
69. Macke RJ, Consolmagno GJ, Britt DT (2011) Density, porosity, and magnetic susceptibility of carbonaceous chondrites. *Meteoritics* 46:1842–1862.
70. El Abassi D, Ibhi A, Faiz B, Aboudaoud I (2013) A simple method for the determination of the porosity and tortuosity of meteorites with ultrasound. *J Geophys Eng* 10:055003.
71. Baaske P, et al. (2007) Extreme accumulation of nucleotides in simulated hydrothermal pore systems. *Proc Natl Acad Sci USA* 104:9346–9351.
72. Domenico PA, Palciauskas VV (1973) Theoretical analysis of forced convective heat transfer in regional ground-water flow. *Geol Soc Am Bull* 84:3803–3814.
73. Sheremet MA (2013) Mathematical simulation of nonstationary regimes of natural convection in a cubical enclosure with finite-thickness heat-conducting walls. *J Eng Thermophys* 22:298–308.
74. Otero L, Molina-Garcia AD, Sans PD (2002) Some interrelated thermophysical properties of liquid water and ice. I. A user-friendly modeling review for food high-pressure processing. *Crit Rev Food Sci Nutr* 42:339–352.
75. Jacobs AFG, Heusinkveld BG, Kraaij A, Paaijmans KP (2008) Diurnal temperature fluctuations in an artificial small shallow water body. *Int J Biometeorol* 52:271–280.